

## Control And Modeling Of Doubly Fed Induction Machine For Wind Turbines

Sai Sindhura K, G. Srinivas Rao

Department of Electrical and Electronics Engineering, V.R Siddhartha Engineering College, Kanuru, Vijayawada-07, Krishna District, Andhra Pradesh, India

### ABSTRACT

Wind power is the most reliable and developed renewable energy source. The share of wind power with respect to total installed power capacity is increasing worldwide. The doubly fed induction generator is an important type of wind generator (WG) due to its robustness and versatility. Its accurate and efficient modeling is very important in distribution system planning and analysis studies. This paper deals with the analysis, modeling and control of a grid connected doubly fed induction generator (DFIG) wind turbine. A mathematical model is derived for modeling of doubly fed induction generator wind turbines. And a control structure using standard proportional integral PI controller and a field-oriented control strategy based on a reference frame rotating synchronously with the rotor flux for variable speed wind turbines using doubly fed induction generator and for attaining injected rotor voltages is described and simulated.

The modeling of the machine considers operating conditions below and above synchronous speed, which are actually accomplished by means of double sided converters joining the machine rotor to the grid. The control strategy successfully decouples the active and reactive powers generated by the machine.

**Keywords** – Active and Reactive Powers, DFIG, Grid side Converter (GSC), Rotor Side Converter (RSC), StatorFluxOrientedcontrol

### I. INTRODUCTION

Wind energy is one of the most important and promising source of renewable energy all over the world, mainly because it reduces the environmental pollution caused by traditional power plants as well as the dependence on fossil fuel, which have limited reserves. Electric energy, generated by wind power plants is the fastest developing and most promising renewable energy source. Off-shore wind power plants provide higher yields because of better conditions. With increased penetration of wind power into electrical grids, wind turbines are largely deployed due to their variable speed feature and hence influencing system dynamics. But unbalances in wind energy are highly impacting the energy conversion and this problem can be overcome by using a Doubly Fed Induction Generator (DFIG).

Doubly fed wound rotor induction machine with vector control is very attractive to the high performance variable speed drive and generating applications. In variable speed drive application, the so called slip power recovery scheme is a common practice here the power due to the rotor slip below or above synchronous speed is recovered to or supplied from the power source resulting in a highly efficient variable speed system. Slip power control can be obtained by using popular Static Scherbius drive for bi directional power flow. The major advantage of the DFIG is that the power electronic equipment used i.e. a back to back converter that handles a fraction of (20-30%) total system power. The back to back converter

consists of two converters i.e. Grid Side Converter (GSC) and Rotor Side Converter (RSC) connected back to back through a dc link capacitor for energy storage purpose. In this paper a control strategy is presented for DFIG and Stator Active and Reactive power control principle is also presented. In order to decouple the active and reactive powers Stator Flux Oriented control is used and hence the induction machine model is developed. The grid side converter and the rotor side converter are used for the control of the active and reactive powers and various wind speed applications. The simulation model is developed and implemented using MATLAB/SIMULINK software.

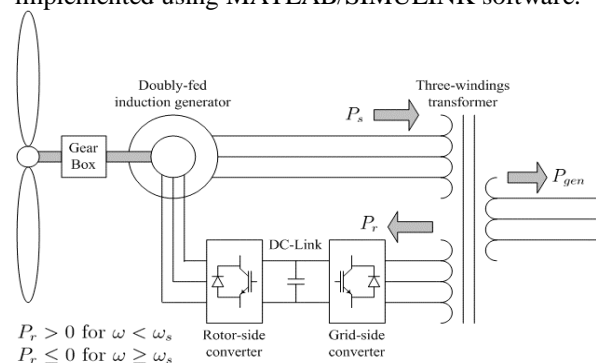


Fig 1. DFIG driven by wind turbine

### II. WIND TURBINE MODEL

Wind turbines produce electricity by using the power of the wind to drive an electrical generator. Wind passes over the blades, generating lift and

exerting a turning force. The rotating blades turn a shaft inside the nacelle, which goes into a gearbox. The gearbox increases the rotational speed to that which is appropriate for the generator, which uses magnetic fields to convert the rotational energy into electrical energy

The power contained in the wind is given by the kinetic energy of the flowing air mass per unit time. That is

$$P_{air} = \frac{1}{2}(\text{air mass per unit time})(\text{wind velocity})^2$$

$$= \frac{1}{2}(\rho AV_{\infty}^3)(V_{\infty}^2)$$

$$= \frac{1}{2} \rho AV_{\infty}^3 \tag{1}$$

Where  $P_{air}$  is the power contained in wind (in watts),  $\rho$  is the air density (1.225 kg/m<sup>3</sup> at 15°C and normal pressure),  $A$  is the swept area in (square meter), and  $V_{\infty}$  is the wind velocity without rotor interference, i.e., ideally at infinite distance from the rotor (in meter per second).

Although Eq. (1.1) gives the power available in the wind, the power transferred to the wind turbine rotor is reduced by the power coefficient,  $C_p$

$$C_p = \frac{P_{wind turbine}}{P_{air}} \tag{2}$$

$$P_{wind turbine} = C_p * P_{air} = \frac{1}{2} C_p \rho A V_{\infty}^3 \tag{3}$$

A maximum value of  $C_p$  is defined by the Betz limit, which states that a turbine can never extract more than 59.3% of the power from an air stream. In reality, wind turbine rotors have maximum  $C_p$  values in the range 25-45%.

It is also conventional to define a tip speed ratio  $\lambda$  as

$$\lambda = \frac{\omega R}{V_{\infty}} \tag{4}$$

Where  $\omega$  is rotational speed of rotor (in rpm),  $R$  is the radius of the swept area (in meter). The tip speed ratio  $\lambda$  and the power coefficient  $C_p$  are the dimensionless and so can be used to describe the performance of any size of wind turbine rotor.

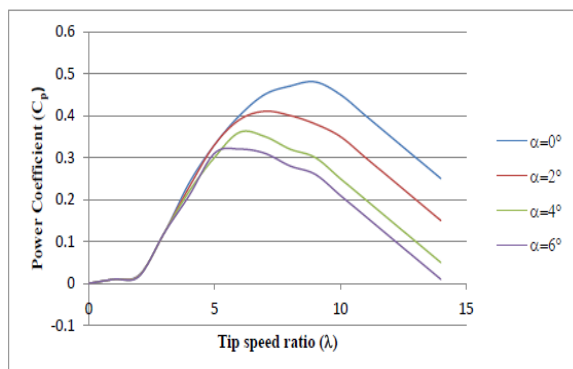


Fig 2. The typical curves of  $C_p$  versus  $\lambda$  for various values of the pitch angle  $\alpha$

### III. DOUBLY FED INDUCTION GENERATOR

#### 3.1 Principle of operation

The WRIM is a conventional 3-phase wound rotor induction machine. The machine stator winding is directly connected to the grid and the rotor winding is connected to the rotor-side VSC by slip rings and brushes. A wide range of variable speed operating mode can be achieved by applying a controllable voltage across the rotor terminals. This is done through the rotor-side VSC. The applied rotor voltage can be varied in both magnitude and phase by the converter controller, which controls the rotor currents. The rotor side VSC changes the magnitude and angle of the applied voltages and hence decoupled control of real and reactive power can be achieved.

### IV. DYNAMIC MODELING OF DFIG

The dynamic analysis of the symmetrical induction machines in the arbitrary reference frame has been intensively used as a standard simulation approach from which any particular mode of operation may then be developed. Matlab/Simulink has an advantage over other machine simulators in modeling the induction machine using dq0 axis transformation [8, 9]. It can be a powerful technique in implementing the machine equations as they are transferred to a particular reference frame. Thus, every single equation among the model equations can be easily implemented in one block so that all the machine variables can be made available for control and verification purposes

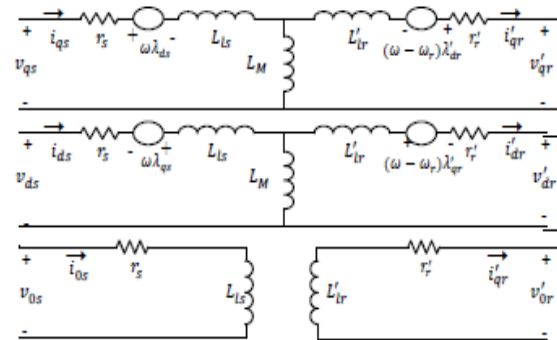


Fig 3. The dq0 equivalent circuit of an induction motor

Driving the model equations can be generated from the dq0 equivalent circuit of the induction machine shown in figure 3. The voltage and flux linkages equations associated with this circuit can be found as follows:

$$v_{qs} = \frac{R_s}{X_{ls}} (\psi_{qs} - \psi_{qm}) + \frac{1}{\omega_b} \frac{d}{dt} \psi_{qs} + \frac{\omega_s}{\omega_b} \psi_{ds} \tag{5}$$

$$v_{ds} = \frac{R_s}{X_{ls}} (\psi_{ds} - \psi_{dm}) + \frac{1}{\omega_b} \frac{d}{dt} \psi_{ds} - \frac{\omega_s}{\omega_b} \psi_{qs} \tag{6}$$

$$v_{qr} = \frac{R_r}{X_{lr}} (\psi_{qr} - \psi_{qm}) + \frac{1}{\omega_b} \frac{d}{dt} \psi_{qr} + \frac{(\omega_s - \omega_r)}{\omega_b} \psi_{dr} \tag{7}$$

$$v_{dr} = \frac{R_r}{X_{lr}}(\psi_{dr} - \psi_{dm}) + \frac{1}{\omega_b} \frac{d}{dt} \psi_{dr} + \frac{(\omega_s - \omega_r)}{\omega_b} \psi_{qr} \quad (8)$$

Flux linkage equations.

$$\frac{d\psi_{qs}}{dt} = \omega_b \left\{ v_{qs} - \frac{\omega_s}{\omega_b} \psi_{ds} - \frac{R_s}{X_{ls}} (\psi_{qs} - \psi_{qm}) \right\} \quad (9)$$

$$\frac{d\psi_{ds}}{dt} = \omega_b \left\{ v_{ds} + \frac{\omega_s}{\omega_b} \psi_{qs} - \frac{R_s}{X_{ls}} (\psi_{ds} - \psi_{dm}) \right\} \quad (10)$$

$$\frac{d\psi_{qr}}{dt} = \omega_b \left\{ v_{qr} - \frac{(\omega_s - \omega_r)}{\omega_b} \psi_{dr} - \frac{R_r}{X_{lr}} (\psi_{qr} - \psi_{qm}) \right\} \quad (11)$$

$$\frac{d\psi_{dr}}{dt} = \omega_b \left\{ v_{dr} + \frac{(\omega_s - \omega_r)}{\omega_b} \psi_{qr} - \frac{R_r}{X_{lr}} (\psi_{dr} - \psi_{dm}) \right\} \quad (12)$$

Where,

$$\psi_{qm} = \frac{X_{sq}}{X_{ls}} \psi_{qs} + \frac{X_{sq}}{X_{lr}} \psi_{qr} \quad (13)$$

$$\psi_{dm} = \frac{X_{sq}}{X_{ls}} \psi_{ds} + \frac{X_{sq}}{X_{lr}} \psi_{dr} \quad (14)$$

$$X_{sq} = \frac{1}{\left(\frac{1}{X_m} + \frac{1}{X_{ls}} + \frac{1}{X_{lr}}\right)} \quad (15)$$

Then substituting the values of the flux linkages to find the currents,

$$i_{qs} = \frac{\psi_{qs} - \psi_{qm}}{X_{ls}} \quad (16)$$

$$i_{qr} = \frac{\psi_{qr} - \psi_{qm}}{X_{lr}} \quad (17)$$

$$i_{ds} = \frac{\psi_{ds} - \psi_{dm}}{X_{ls}} \quad (18)$$

$$i_{dr} = \frac{\psi_{dr} - \psi_{dm}}{X_{lr}} \quad (19)$$

Based on the above equations, the torque and rotor speed can be determined as follows,

$$T_s = \frac{3P}{2} \frac{1}{\omega_b} (\psi_{ds} i_{qs} - \psi_{qs} i_{ds}) \quad (20)$$

$$\omega_r = \int \frac{P}{2J} (T_s - T_l) \quad (21)$$

The active and reactive powers are obtained by using equations

$$P_s = \frac{-3}{2} [v_{qs} i_{qs} + v_{ds} i_{ds}] \quad (22)$$

$$Q_s = \frac{-3}{2} [v_{qs} i_{ds} - v_{ds} i_{qs}] \quad (23)$$

$$P_r = \frac{-3}{2} [v_{qr} i_{qr} + v_{dr} i_{dr}] \quad (24)$$

$$Q_r = \frac{-3}{2} [v_{qr} i_{dr} - v_{dr} i_{qr}] \quad (25)$$

The three-phase stator voltages of an induction machine under balanced conditions can be expressed as:

$$V_a = \sqrt{2} V_{rms} \sin(\omega t) \quad (26)$$

$$V_b = \sqrt{2} V_{rms} \sin(\omega t - 120) \quad (27)$$

$$V_c = \sqrt{2} V_{rms} \sin(\omega t + 120) \quad (28)$$

These three-phase voltages are transferred to a synchronously rotating reference frame in only two phases (d-q axis transformation). This can be done using the following two equations.

$$\begin{bmatrix} v_a \\ v_b \\ v_c \end{bmatrix} = \begin{bmatrix} \cos\theta & -\sin\theta \\ \cos(\theta - 120) & -\sin(\theta - 120) \\ \cos(\theta + 120) & -\sin(\theta + 120) \end{bmatrix} \begin{bmatrix} v_d \\ v_q \end{bmatrix} \quad (29)$$

The two phase currents (d-q axis) are transferred to three phase using the below equation

$$\begin{bmatrix} i_d \\ i_q \end{bmatrix} = \frac{2}{3} \begin{bmatrix} \cos\theta & \cos(\theta - 120) & \cos(\theta + 120) \\ -\sin\theta & -\sin(\theta - 120) & -\sin(\theta + 120) \end{bmatrix} \begin{bmatrix} i_a \\ i_b \\ i_c \end{bmatrix} \quad (30)$$

## V. CONTROL SCHEME

The DFIM control structure shown in Fig. 4 contains two cascaded control-loops. The outer one governs both the stator side active and reactive powers, so that the power factor set point value demanded by the electric energy distribution company is complied with as accurately as possible. Simultaneously, it would be convenient to employ profitably the whole active power generation capability provided by the wind at each moment, from the income-yield capacity point of view. On the other hand, the inner control-loop task consists in controlling independently the rotor current direct  $i_{rd}$  and quadrature  $i_{rq}$  components expressed according to the reference frame fixed to the stator flux-linkage space phasor. In order to implement this inner control-loop, the stator-flux-oriented vector control method based on two identical PI controllers is used.

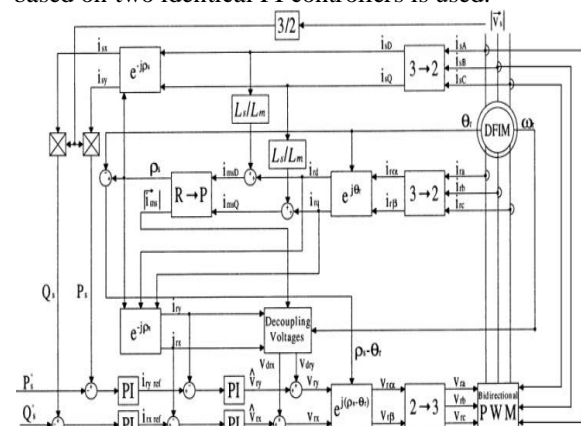


Fig 4. Overall control structure of DFIM

### 5.1 Vector Control Implementation

As stated in (9) and (10), when governing a stator-flux-oriented vector-controlled generator, it can

be proved that variations in rotor current real and imaginary components  $i_{rx}$ ,  $i_{ry}$  are directly reflected on their corresponding stator current components  $i_{sx}$ ,  $i_{sy}$  provided that they are all referred to the reference frame fixed to the stator flux-linkage space phasor [8]. Therefore, and are used to control the stator reactive and active powers, respectively. Thus, the steps followed to model and implement this vector control algorithm are described below and can also be identified in Fig. 4.

1) Converting Three phase to two phase of both stator and rotor side currents by using Clarke's transformation

2) Estimation of the stator flux-linkage space phasor  $\rho_s$  angular position with respect to the stationary direct axis. Because the rotor side current components are to be changed first from their natural axes to the stationary reference frame, it is important to measure the rotor angle. The equations to be followed are given next

$$i_{rd} = i_{r\alpha} \cos \theta_r - i_{r\beta} \sin \theta_r \quad (31)$$

$$i_{rq} = i_{r\alpha} \sin \theta_r + i_{r\beta} \cos \theta_r \quad (32)$$

$$i_{msD} = \frac{L_s}{L_m} i_{sd} + i_{rd} \quad (33)$$

$$i_{msQ} = \frac{L_s}{L_m} i_{sq} + i_{rq} \quad (34)$$

$$\rho_s = \arctan \frac{i_{msQ}}{i_{msD}} \quad (35)$$

3) Based on the errors in both compared current quantities i.e.,  $i_{rx}$  and  $i_{ry}$  with their corresponding  $i_{rxref}$ ,  $i_{ryref}$  set-point values we get the voltage components  $\hat{V}_{rx}$  and  $\hat{V}_{ry}$  which are to be applied to the rotor side are generated by means of two identical PI controllers, as shown below

$$i_{rx} = i_{rd} \cos \rho_s + i_{rq} \sin \rho_s \quad (36)$$

$$i_{ry} = i_{rd} \sin \rho_s - i_{rq} \cos \rho_s \quad (37)$$

$$\hat{V}_{rx} = K_p (b i_{rxref} - i_{rx}) + K_i \int_0^t (i_{rxref} - i_{rx}) dt \quad (38)$$

$$\hat{V}_{ry} = K_p (b i_{ryref} - i_{ry}) + K_i \int_0^t (i_{ryref} - i_{ry}) dt \quad (39)$$

The PI controllers used in Simulink are discrete PI controllers

4) In order to improve the decoupling between x & y axes, the  $V_{drx}$  and  $V_{dry}$  decoupling voltage components given below are added to  $\hat{V}_{rx}$  and  $\hat{V}_{ry}$  respectively.

$$V_{drx} = -\omega_{sl} L'_r i_{ry} \quad (40)$$

$$V_{dry} = \omega_{sl} (L_r - L'_r) \overline{i_{ms}} + \omega_{sl} L'_r i_{rx} \quad (41)$$

Where,

$$L'_r = L_r - \left( \frac{L_m^2}{L_s} \right) \quad (42)$$

$$\omega_{sl} = 2\pi f_s - \omega_r \quad (43)$$

$$|\overline{i_{ms}}| = \sqrt{i_{msD}^2 + i_{msQ}^2} \quad (44)$$

The resultant voltages in both axes will be referred to  $V_{rx}$  as and  $V_{ry}$

5) Expression for  $V_{rx}$  and  $V_{ry}$  according to the rotor natural reference frame as follows.

$$V_{r\alpha} = V_{rx} \cos(\rho_s - \theta_r) - V_{ry} \sin(\rho_s - \theta_r) \quad (45)$$

$$V_{r\beta} = V_{rx} \sin(\rho_s - \theta_r) + V_{ry} \cos(\rho_s - \theta_r) \quad (46)$$

6) By using Inverse Clarke's transformation the rotor three phase voltages are obtained from two phase to three phase

## 5.2 Grid side controller

The grid side voltage source controller provides regulation of voltage of DC bus capacitor and also provides control of the reactive power and also adjusts the power factor on grid side. The grid side VSC acts as rectifier at sub-synchronous speeds and as inverter during super-synchronous speeds

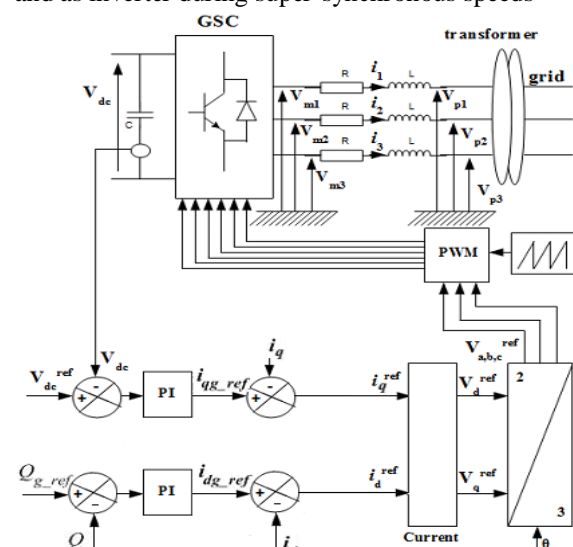


Fig 5. Control Structure of Grid Side Converter Control.

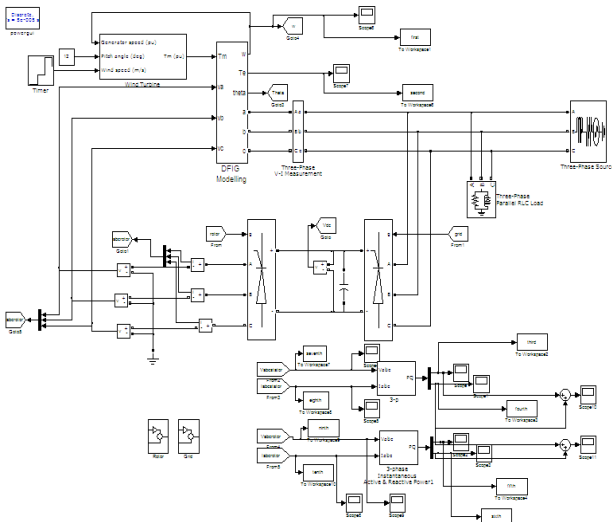


Fig 6. Matlab/simulink diagram of DFIM

**VI. RESULTS AND DISCUSSIONS**

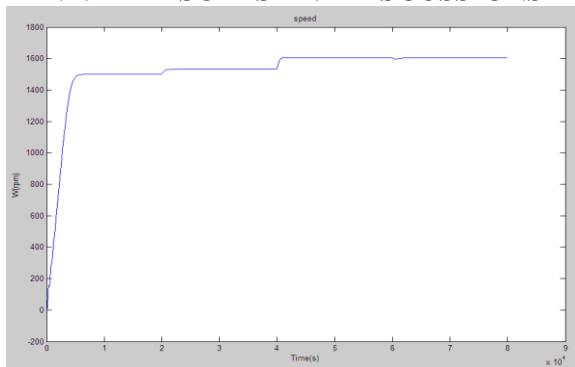


Fig 6. Speed  $\omega$

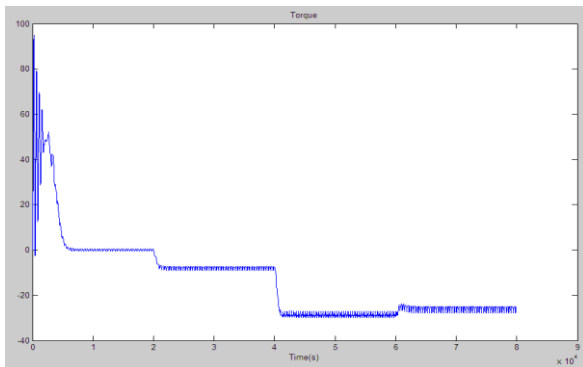


Fig 7. Torque  $T_m$

Below synchronous speed the torque is positive and the machine acts as motor, above synchronous speed the torque is negative and machine acts as generator equal to synchronous speed the torque is zero

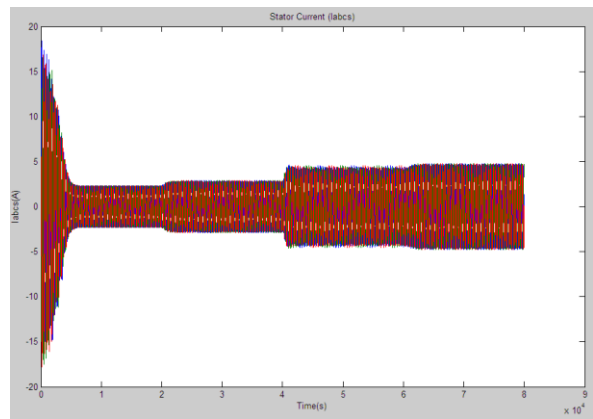


Fig 8. Stator current  $I_{abc}$

Even when the speed equal to synchronous speed the stator produces current and as the speed increases then the stator current also tends to increase.

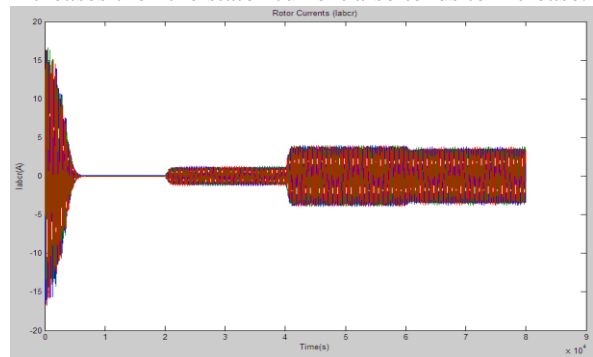


Fig 9. Rotor currents  $I_{abc}$

When speed equal to synchronous speed rotor current is zero and as the speed increases the rotor current also increases.

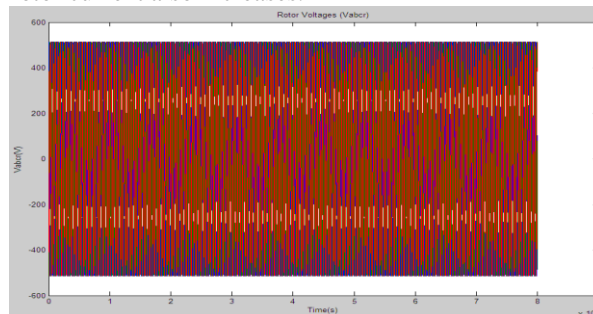
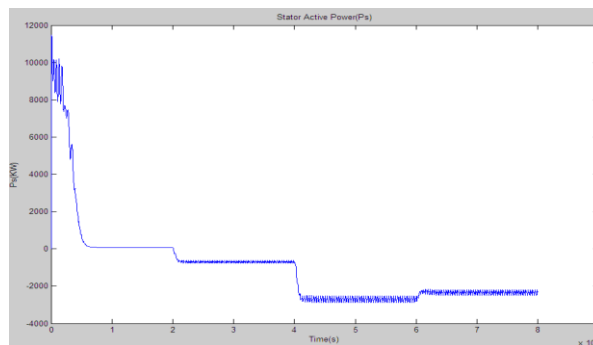


Fig 10. Rotor voltages



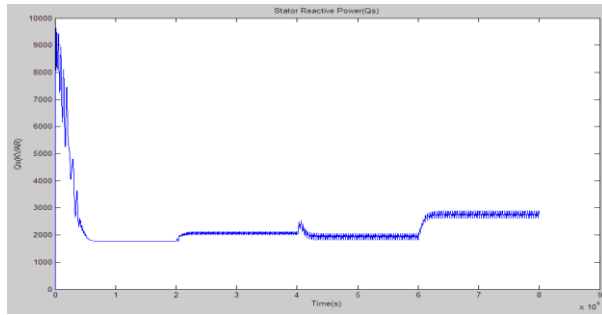


Fig 11. Stator Active and Reactive powers ( $P_s, Q_s$ )

Here the stator active power is negative which means that the active power is send from stator to the grid

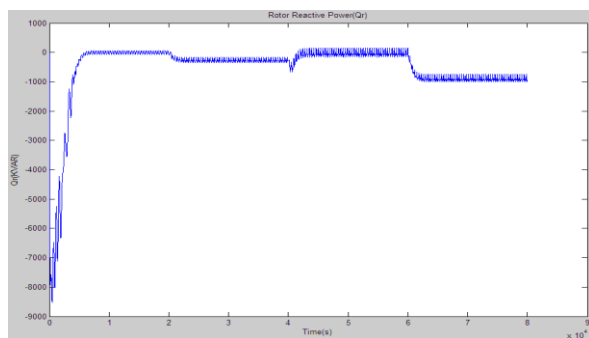
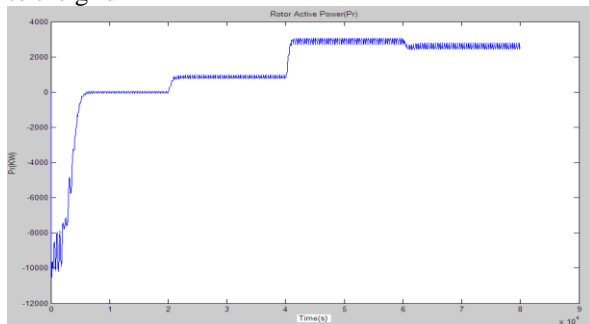
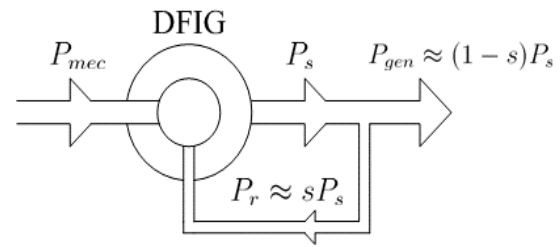


Fig 12. Rotor Active and Reactive powers ( $P_r, Q_r$ )

Generally the absolute value of slip is much lower than 1 and, consequently,  $P_r$  is only a fraction of  $P_s$ . Since  $T_m$  is positive for power generation and since  $\omega_s$  is positive and constant for a constant frequency grid voltage, the sign of  $P_r$  is a function of the slip sign.  $P_r$  is positive for negative slip (speed greater than synchronous speed) and it is negative for positive slip (speed lower than synchronous speed). For super-synchronous speed operation,  $P_r$  is transmitted to DC bus capacitor and tends to rise the DC voltage. For sub-synchronous speed operation,  $P_r$  is taken out of DC bus capacitor and tends to decrease the DC voltage



$s > 0$  Sub-synchronous speed  
 $s \leq 0$  Super-synchronous speed

Fig 13. Active-power flows in the Doubly-fed Induction machine.

#### Wound Rotor Induction Machine

Parameters:-

|                         |                           |
|-------------------------|---------------------------|
| Nominal Power           | $P_n = 7.5 \text{ Kw}$    |
| Stator Voltage          | $V_s = 415 \text{ V}$     |
| Stator Frequency        | $f_s = 50 \text{ Hz}$     |
| Stator Resistance       | $R_s = 7.83 \Omega$       |
| Stator Inductance       | $L_s = 0.4751 \text{ H}$  |
| Rotor Resistance        | $R_r = 7.55 \Omega$       |
| Rotor Inductance        | $L_r = 0.4751 \text{ H}$  |
| Mutual Inductance       | $L_m = 0.4535 \text{ H}$  |
| Inertia Constant        | $J = 0.06 \text{ Kg-m}^2$ |
| Number of Pair of Poles | $P = 2$                   |
| Rating Speed            | $N_r = 1440 \text{ rpm}$  |

## VII. CONCLUSION

This paper presents the doubly fed induction generator used in variable-speed wind power generation. And a control structure using standard proportional integral PI controller and a field-oriented control strategy based on a reference frame rotating synchronously with the rotor flux for variable speed wind turbines using doubly fed induction generator and for obtaining injected rotor voltages is described and simulated. Hence results are determined sub-synchronous, super synchronous and synchronous speeds and the active and reactive power control is achieved by the RSC and GSC. For the purpose of future extension instead of standard PI controllers fuzzy controllers etc. can be used.

## NOMENCLATURE

|                  |   |
|------------------|---|
| $v_s, v_r$       | Stator and rotor voltages                       |
| $i_s, i_r$       | Stator and rotor currents                       |
| $\psi_s, \psi_r$ | Stator and rotor flux linkages                  |
| $L_m, X_m$       | Machine magnetizing inductance, Reactance       |
| $L_s, L_r$       | Stator and rotor per phase winding inductances  |
| $L_{ls}, L_{lr}$ | Stator and rotor per phase leakage inductances  |
| $R_s, R_r$       | Stator and rotor per phase winding resistances  |
| $\sigma$         | Leakage factor                                  |
| $S_s, S_r$       | Stator and rotor apparent power                 |
| $P_s, P_r$       | Stator and rotor active power                   |
| $Q_s, Q_r$       | Stator and rotor reactive power                 |
| $P_n, Q_n$       | Wind Turbine net active & reactive powers       |
| $f_s$            | Grid frequency                                  |
| $i_{ms}$         | Stator magnetizing current space phasor modulus |

$|\bar{i}_r|$  Rotor current space phasor modulus  
 $P_{sref}$  Stator side active power reference value  
 $Q_{sref}$  Stator side reactive power reference value  
 $i_{rx}, i_{ry}$  Direct- and quadrature-axis rotor current components respectively expressed in the stator-flux-oriented reference frame  
 $i_{rxref}, i_{ryref}$  Reference values of the rotor current components, respectively  
 $i_{r\alpha}, i_{r\beta}$  Direct- and Quadrature – axis rotor current components respectively expressed in the rotor natural reference frame  
 $i_{sD}, i_{sQ}$  Direct – and quadrature- axis stator current components respectively, expressed in the stationary reference frame  
 $i_{sx}, i_{sy}$  Direct – and quadrature – axis stator current components respectively, expressed in the stator- flux-oriented reference frame  
 $k_p, k_i$  Inner loop vector controller PI compensator parameters  
 $k_{p1}, k_{i1}$  Outer loop vector controller PI compensator parameters  
 $i_{msD}, i_{msQ}$  Direct- quadrature-axis stator magnetizing current components respectively, expressed in the stationary reference frame  
 $v_{drx}, v_{dry}$  Direct- and quadrature- axis rotor decoupling voltage components, respectively, expressed in the stator- flux- oriented reference frame  
 $v_{rx}, v_{ry}$  Direct- and quadrature- axis rotor voltage components, respectively, expressed in the stator-flux- oriented reference frame  
 $v_{r\alpha}, v_{r\beta}$  Direct- and quadrature- axis rotor voltage components, respectively, expressed in the rotor natural reference frame  
 $|\bar{i}_s|$  Stator voltage space phasor modulus  
 $v_{sD}, v_{sQ}$  Direct- and quadrature- axis stator voltage components, respectively, expressed in the stationary reference frame  
 $\rho_s$  Phase angle of stator flux- linkage space phasor with respect to the direct – axis of the stationary reference frame  
 $\omega_{sl}$  Angular slip frequency  
 $v_{rD}, v_{rQ}$  Direct- and quadrature- axis rotor voltage components, respectively, expressed in the stationary reference frame  
 $v_{dcref}$  DC Link Voltage Reference Value  
 $i_{qref}$  Quadrature axis reference current  
 $v_{as}$  Stator voltage at Phase A  
 $v_{bs}$  Stator voltage at Phase B  
 $v_{cs}$  Stator voltage at Phase C

SUFFICES, SUPERSRIPTS  
 s, r Stator, rotor  
 $\alpha, \beta$   $\alpha, \beta$  Stationary reference frame  
 d, q d-q reference frame  
 x, y x, y stator-flux-oriented reference frame

a, b, c Three-phase reference

**REFERENCES**

- [1] Srinath Vanukuru, Sateesh Sukhavasi, “Active & Reactive Power Control Of A Doubly Fed Induction Generator Driven By A Wind Turbine”, International Journal of Power System Operation and Energy Management, ISSN (PRINT): 2231–4407, Volume-1, Issue-2, 2011
- [2] Arantxa Tapia, Gerardo Tapia, J. Xabier Ostolaza, “Modeling and Control of a Wind Turbine Driven doubly fed Induction Generator”, IEEE 2003. (reference2).
- [3] A. Peterson “Analysis, Modeling and Control of Doubly fed Induction Generators for Wind Turbines,” in Energy and Environment. 2005, PhD Dissertation thesis, Chalmers University of Technology:
- [4] A. Tapia “Modeling and Control of a wind turbine driven doubly fed induction generator.” Energy Conversion, IEEE Transaction on, 2003, 194-204.
- [5] D.J. Atkinson, R.A. Larkin, and R. Jones, “A vector-controlled doubly- fed induction generator for a variable- speed wind turbine application,” Trans, Inst, Meas, Contr., vol.19, no. 1, 2-12,1997.
- [6] I.P.Kopilov, ‘Mathematical Simulation of Electrical Machines’, VishayaShcola, Moscow, 1987.
- [7] R.S. Pena, J.C. Clare, and G.M. Asher, “Vector control of a variable speed doubly-fed induction machine for wind generation system, EPEJ” vol. 6, no 3-4, 60-67, Dec.1996.
- [8] R. Pena, J.C. Clare, G.M. Asher, “Double fed Induction generator using back-to-back PWM converters and its application to variable-speed wind-energy generation”. Electric Power Applications, IEE Proceedings 1996. 143(3),231-241
- [9] A. Miller, E. Muljadi, and D. Zinger, “A variable speed wind turbine power control,” IEEE Trans. Energy Conversion, vol. 12, pp. 181–186, June 1997.
- [10] D. J. Atkinson, R. A. Lakin, and R. Jones, “A vector-controlled doubly-fed induction generator for a variable-speed wind turbine application,” Trans. Inst. Meas. Contr., vol. 19, no. 1, pp. 2–12, 1997.
- [11] J.B.Ekanayake, ‘Control of Doubly Fed Induction Generator Wind Turbines’, IEE Power Engineer, Feb. 2003.